

LncRNA MIF-AS1 aggravates the progression of ovarian cancer by sponging miRNA-31-5p

Y. FAN¹, L. WANG², X.-C. HAN¹, H.-Y. MA¹, N. ZHANG¹, L. ZHE¹

¹Department of Gynecology, People's Hospital of Ningxia Hui Autonomous Region, Yinchuan, China

²Ningxia Medical University, Yinchuan, China

Abstract. – **OBJECTIVE:** The aim of this study was to uncover the role of lncRNA MIF-AS1 in influencing the biological phenotypes of ovarian cancer (OC) and the underlying mechanism.

PATIENTS AND METHODS: OC tissues and adjacent normal tissues were collected from 50 OC patients. The expression level of lncRNA MIF-AS1 in OC tissues and cells was determined by quantitative Real-Time Polymerase Chain Reaction (qRT-PCR). The prognostic potential of MIF-AS1 in OC patients was assessed by the Kaplan-Meier method. Subsequently, the regulatory effects of MIF-AS1 on proliferative, migratory, and invasive abilities of ES-2 and HO-8910 cells were evaluated by a series of functional experiments. Dual-Luciferase reporter gene assay, qRT-PCR, and Western blot were further conducted to verify the interaction in the regulatory loop MIF-AS1/miRNA-31-5p/PLCB1.

RESULTS: MIF-AS1 was significantly upregulated in OC tissues and cell lines ($p < 0.05$). Higher level of MIF-AS1 predicted significantly worse prognosis of OC patients ($p < 0.05$). The knockdown of MIF-AS1 markedly attenuated the proliferative, migratory, and invasive abilities of ES-2 and HO-8910 cells ($p < 0.05$). Dual-Luciferase reporter gene assay verified that MIF-AS1 competed with PLCB1 to bind miRNA-31-5p. In addition, MIF-AS1 negatively regulated miRNA-31-5p expression cells, and miRNA-31-5p negatively regulated PLCB1 expression in OC.

CONCLUSIONS: MIF-AS1 was significantly upregulated in OC, which accelerated the proliferative, migratory, and invasive abilities of OC cells. Furthermore, the regulatory loop MIF-AS1/miRNA-31-5p/PLCB1 could be utilized as a therapeutic target for OC.

Key Words:

Ovarian cancer (OC), MIF-AS1, Proliferation, Migration, Invasion.

Introduction

Ovarian cancer (OC) is one of the most common malignant tumors in the female reproductive system, seriously affecting women's health. Currently, the mortality of OC ranks first among all kinds of gynecological malignancies. About 70% of OC patients have already been diagnosed in the advanced stage, whose postoperative recurrence is extremely prevalent^{1,2}. Although great progress has been made in therapeutic approaches, the 5-year survival of OC patients remains lower than 30%^{3,4}. Meanwhile, the therapeutic efficacy of advanced OC is far from satisfactory. Therefore, exploring the pathogenesis of OC and searching for tumor hallmarks are of significance for improving the clinical outcome of OC patients.

Long non-coding RNAs (lncRNAs) are a type of non-coding RNAs with over 200 nt in length. They do not encode proteins but participate in the crucial regulations on gene expression⁵. Through complementary base pairing, lncRNAs result in function decline of microRNAs (miRNAs) by absorbing them⁶. Besides, the interaction of lncRNA-DNA influences the epigenetics of genes⁷. In recent years, critical functions of lncRNAs have been identified in multiple malignant tumors. In prostate cancer, the regulatory loop lncRNA SNHG15/miR-338-3p/FKBP1A axis aggravates its progression⁸. lncRNA HEIH suppresses the miR-200b/a/429 axis, thus triggering the proliferation and metastasis of melanoma⁹. Accumulating evidence has demonstrated the involvement of lncRNAs in OC progression¹⁰. lncRNA H19 induces epithelial-mesenchymal transition (EMT) in OC cells by serving as a miR-370-3p sponge to upregulate the transforming growth factor- β (TGF- β)¹¹. lncRNA MEG3 upregulates EGFR by sponging miR-219a-5p, thus activating

EMT in OC¹². Furthermore, lncRNA MIF-AS1 is highly expressed in various malignancies, exerting crucial functions in tumor progression^{13,14}.

The aim of this study was to investigate the expression level of MIF-AS1 and its biological function in OC. Through functional experiments, the regulatory loop MIF-AS1/miRNA-31-5p/PLCB1 was identified to influence the malignant progression of OC.

Patients and Methods

Patients and OC Samples

OC tissues and adjacent normal tissues were surgically resected from 50 OC patients. All patients were pathologically diagnosed. The collected tissue samples were preserved at -80°C for use. None of the enrolled patients received preoperative anti-tumor therapy. Meanwhile, they did not have the history of other malignancies. Follow-up data were collected from OC patients. Informed consent was obtained from patients and their families. This study was approved by the Ethics Committee of People's Hospital of Ningxia Hui Autonomous Region.

Cell Culture and Transfection

Ovarian epithelial cells (IOSE80) and OC cells (OC3, HO-8910, ES-2, and SKOV-3) were provided by Cell Bank (Shanghai, China). All cells were cultured in Roswell Park Memorial Institute-1640 (RPMI-1640; HyClone, South Logan, UT, USA) containing 10% fetal bovine serum (FBS; HyClone, South Logan, UT, USA), and 1% penicillin-streptomycin in a 5% CO₂ incubator at 37°C. Culture medium was daily replaced. Cell passage was conducted at 70% of confluence.

The cells were pre-seeded into 6-well plates at 30-40% of confluence. Cell transfection was performed according to the instructions of Lipofectamine 2000 (Invitrogen, Carlsbad, CA, USA). Fresh medium was replaced at 24 h. The transfection vectors were provided by GenePharma (Shanghai, China).

RNA Extraction and Quantitative Real-Time Polymerase Chain Reaction (qRT-PCR)

The total RNA in cells was extracted using the TRIzol method (Invitrogen, Carlsbad, CA, USA). Subsequently, extracted RNAs were reverse transcribed to cDNAs according to the instructions of PrimeScript RT reagent kit (TaKaRa, Otsu, Shiga, Japan). The RNA concentration was detected using a spectrometer. QRT-PCR was performed in accordance with SYBR Premix Ex Taq™ (TaKaRa, Otsu, Shiga, Japan). The relative level of genes was calculated by the 2^{-ΔΔCt} method. The primer sequences used in this study were listed in Table I.

5-Ethynyl-2'-Deoxyuridine (EdU) Assay

The cells were first inoculated into 96-well plates at a density of 1×10⁵ cells per well. Then, the cells were labeled with 100 μL of EdU reagent (50 μM) per well for 2 h. After washing with phosphate-buffered saline (PBS), the cells were fixed in 50 μL of fixation buffer, decolorized with 2 mg/mL glycine, and permeated with 100 μL of penetrant. After washing with PBS once, the cells were stained with 100 μL of Hoechst33342 in the dark for 30 min. The EdU-positive ratio was determined under a fluorescent microscope (magnification 20×).

Table I. The sequences related to the study.

| Gene | Sequences |
|--------------|----------------------------------|
| miR-31-5p F: | ACACTCCAGCTGGGAGGCAAGATGCTGGCATA |
| miR-31-5p R: | CTCAACTGGTGTCTGGAGTCGGGCAATTCAG |
| MIF-AS1 F: | ACATCGGCATGATGGCAGAA |
| MIF-AS1 R: | TCACAAAAGGCGGGACCAC |
| GAPDH F: | AGCCACATCGCTCAGACAC |
| GAPDH R: | GCCCAATACGACCAAATCC |
| U6 F: | CTCGCTTCGGCAGCACATA |
| U6 R: | CGCTTACGAATTTGCGTG |
| PLCB1 F: | GTTGGCTGGGAACCTCGTCTG |
| PLCB1 R: | CACTCTGCGATGGCTTCTATG |

Wound Healing Assay

The cells were seeded into 6-well plates, with 5.0×10^6 cells/well. An artificial wound was created in the confluent cell monolayer using a 200 μ L pipette tip. Wound closure images were captured at 0 and 24 h using an inverted microscope, respectively. The relative distance of wound healing was finally calculated.

Transwell Assay

Cell density was first adjusted to 1×10^5 cells/ml. 100 μ L of cell suspension was applied in the upper side of the transwell chamber (Corning, Corning, NY, USA) pre-coated with 100 μ L of Matrigel. Meanwhile, 600 μ L of medium containing 20% FBS was applied in the bottom side. After 48 h of incubation, the cells penetrated to the bottom side were fixed with 4% paraformaldehyde for 20 min and stained with crystal violet for 20 min. Next, penetrating cells were observed using a microscope. 5 fields of view were randomly selected for each sample, and the number of penetrating cells was counted (magnification 20 \times).

Dual-Luciferase Reporter Gene Assay

Based on the binding sequences between MIF-AS1 and miRNA-31-5p, as well as between miRNA-31-5p and PLCB1, the wild-type and mutant-type MIF-AS1 or PLCB1 vectors were constructed, respectively. Subsequently, the cells were co-transfected with miRNA-31-5p mimics/negative control and wild-type/mutant-type vector for 48 h. Finally, the cells were lysed, and the relative Luciferase activity was determined (Promega, Madison, WI, USA).

Western Blot

The total protein in cells was extracted using radioimmunoprecipitation assay (RIPA; Beyotime, Shanghai, China). The concentration of the protein samples was quantified by the bicinchoninic acid (BCA) method (Pierce, Rockford, IL, USA). The protein samples were separated by electrophoresis and transferred onto polyvinylidene difluoride (PVDF) membranes (Millipore, Billerica, MA, USA). After blocking in 5% skimmed milk for 2 hours, the membranes were incubated with primary antibodies at 4 $^{\circ}$ C overnight. On the next day, the membranes were incubated with corresponding secondary antibodies for 2 h. Immuno-reactive bands were exposed by enhanced chemiluminescence (ECL) and analyzed by Image Software.

Statistical Analysis

The Statistical Product and Service Solutions (SPSS) 20.0 (IBM Corp., Armonk, NY, USA) was used for all statistical analysis. GraphPad Prism 7 (La Jolla, CA, USA) was utilized for depicting figures. Experimental data were expressed as mean \pm standard deviation ($\bar{x} \pm SD$). The differences between the two groups were compared using the *t*-test. Survival analysis was conducted by the Kaplan-Meier method. $p < 0.05$ was considered statistically significant.

Results

Upregulation of MIF-AS1 in OC

A total of 50 matched OC tissues and adjacent normal tissues were collected in this study. QRT-PCR results revealed a significantly higher abundance of MIF-AS1 in OC tissues ($p < 0.05$; Figure 1A). Consistently, MIF-AS1 was remarkably up-regulated in OC cells relative to ovarian epithelial cells ($p < 0.05$; Figure 1B). Prognostic potential of MIF-AS1 was assessed by the Kaplan-Meier method. The results indicated that the prognosis of OC patients with a higher level of MIF-AS1 was remarkably worse than those with a lower level ($p < 0.05$; Figure 1C).

Knockdown of MIF-AS1 Suppressed the Proliferation of OC

Transfection of si-MIF-AS1 in ES-2 and HO-8910 cells markedly downregulated MIF-AS1 level, presenting a pronounced transfection efficacy ($p < 0.05$; Figure 2A). EdU assay showed significantly reduced EdU-positive ratio in OC cells with MIF-AS1 knockdown ($p < 0.05$; Figure 2B). Besides, the number of visible colonies was remarkably reduced after transfection of si-MIF-AS1 in OC cells ($p < 0.05$; Figure 2C). Hence, we believed that the knockdown of MIF-AS1 attenuated the proliferative ability of OC.

Knockdown of MIF-AS1 Suppressed the Migration and Invasion of OC

Wound distance was significantly shortened in ES-2 and HO-8910 cells transfected with si-MIF-AS1 than those of the controls, suggesting attenuated migratory ability ($p < 0.05$; Figure 3A). In addition, the transwell assay revealed that the number of invasive cells significantly decreased after transfection of si-MIF-AS1 in OC cells ($p < 0.05$; Figure 3B). Therefore, the silence of MIF-AS1 attenuated the metastatic ability of OC cells.

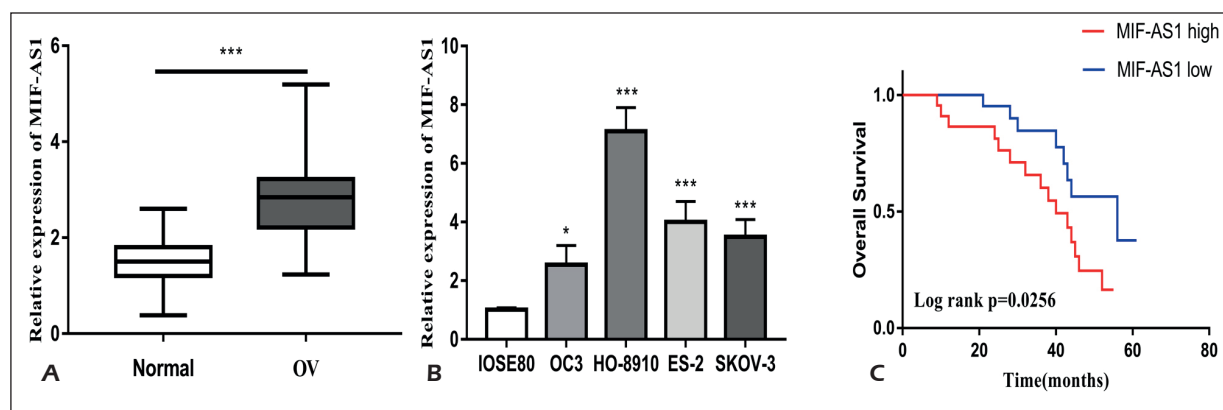


Figure 1. Upregulation of MIF-AS1 in OC. **A**, MIF-AS1 level in OC tissues and matched adjacent normal tissues. **B**, MIF-AS1 level in ovarian epithelial cells (IOSE80) and OC cells (OC3, HO-8910, ES-2, and SKOV-3). **C**, Overall survival in OC patients with high or low level of MIF-AS1. * $p < 0.05$; *** $p < 0.001$.

Interaction in MIF-AS1/ MiRNA-31-5p/PLCB1

Through online bioinformatics analysis, the binding sequences in the promoter regions of MIF-AS1 and miRNA-31-5p were identified (Figure 4A). Subsequently, the Luciferase vectors were constructed based on the binding sequences. Dual-Luciferase reporter gene assay demonstrated that Luciferase activity was markedly declined after co-transfection of wild-type MIF-AS1 vector and miRNA-31-5p mimics ($p < 0.05$; Figure 4C). This verified the binding relationship between MIF-AS1 and miRNA-31-5p. Similarly, the binding sequences between miRNA-31-5p and PLCB1 were discovered (Figure 4B). Dual-Luciferase reporter gene assay further confirmed their binding relationship as well (Figure 4D).

Subsequently, the expression levels of miRNA-31-5p and PLCB1 in OC cells were determined. QRT-PCR revealed that miRNA-31-5p was significantly downregulated, while PLCB1 was upregulated in OC cells relative to ovarian epithelial cells ($p < 0.05$; Figures 4E, 4G). In ES-2 and HO-8910 cells transfected with si-MIF-AS1, miRNA-31-5p expression was markedly upregulated ($p < 0.05$; Figure 4F). Moreover, both the mRNA and protein levels of PLCB1 remarkably decreased in OC cells overexpressing miRNA-31-5p ($p < 0.05$; Figures 4H, 4I). Collectively, the regulatory loop MIF-AS1/miRNA-31-5p/PLCB1 was identified, which was responsible for aggravating the progression of OC.

Discussion

Currently, most OC patients seek medical advice because of abdominal mass or ascites. The detective rate of advanced OC is relatively

high. OC has already become the most common malignancy in the female reproductive system, leading to deaths. Recurrence and chemotherapy-resistance are the therapeutic obstacles for OC, greatly restricting clinical prognosis¹⁵. Therefore, it is urgent to uncover the etiology and pathogenesis of OC.

LncRNAs were initially considered as transcription noise without protein-encoding abilities⁵. In recent years, they have been identified to be abnormally expressed in tumors, presenting regulatory effects on multiple aspects of tumor cell behaviors¹⁶. Currently, the potential role of lncRNAs in OC has been well concerned as well. In breast cancer, lncRNA MIF-AS1 accelerates the proliferation, metastasis, and EMT of tumor cells by targeting the miR1249-3p/HOXB8 axis¹⁴. Through upregulating NDUFA4, MIF-AS1 stimulates the proliferative rate and inhibits the apoptosis of gastric cancer cells¹³. In our paper, MIF-AS1 was significantly upregulated in OC tissues and cells, suggesting a potential involvement of MIF-AS1 in the progression of OC. *In vitro* experiments demonstrated that the knockdown of MIF-AS1 markedly attenuated the proliferative, migratory, and invasive abilities of ES-2 and HO-8910 cells. Therefore, MIF-AS1 might serve as an oncogene to aggravate the malignant progression of OC.

LncRNA has been believed to downregulate the corresponding miRNA by sponging it¹⁷. Here, we predicted the binding sequences in the promoter regions of MIF-AS1 and miRNA-31-5p. In OC cells, MIF-AS1 negatively regulated the expression level of miRNA-31-5p. Moreover, miRNA-31-5p was predicted to bind PLCB1.

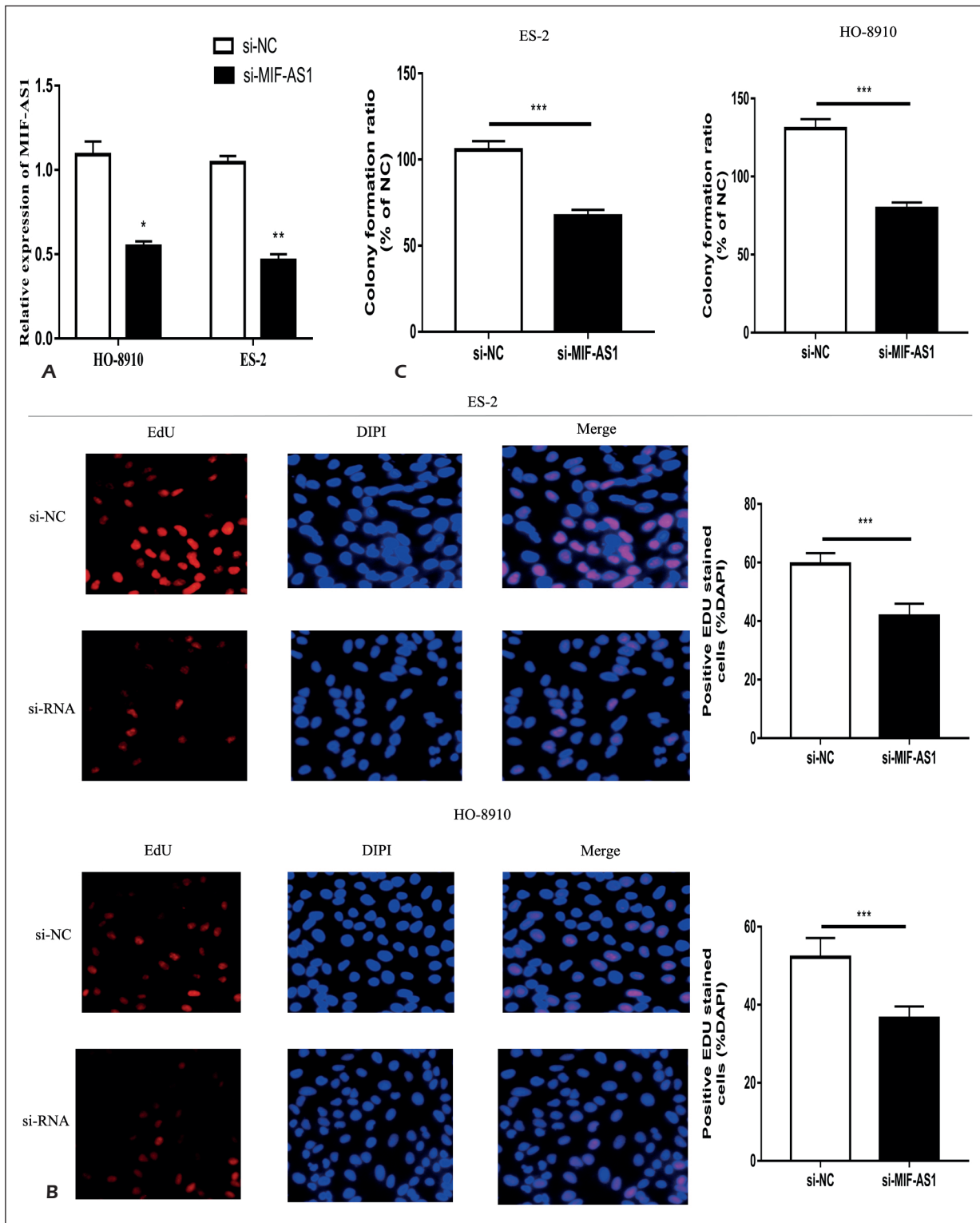


Figure 2. Knockdown of MIF-AS1 suppressed the proliferation of OC. **A**, Transfection efficacy of si-MIF-AS1 in HO-8910 and ES-2 cells. **B**, EdU-positive ratio in HO-8910 and ES-2 cells transfected with si-NC or si-MIF-AS1 (magnification: 20×). **C**, Colony formation ratio in HO-8910 and ES-2 cells transfected with si-NC or si-MIF-AS1 (magnification: 20×). * $p < 0.05$; ** $p < 0.01$; *** $p < 0.001$.

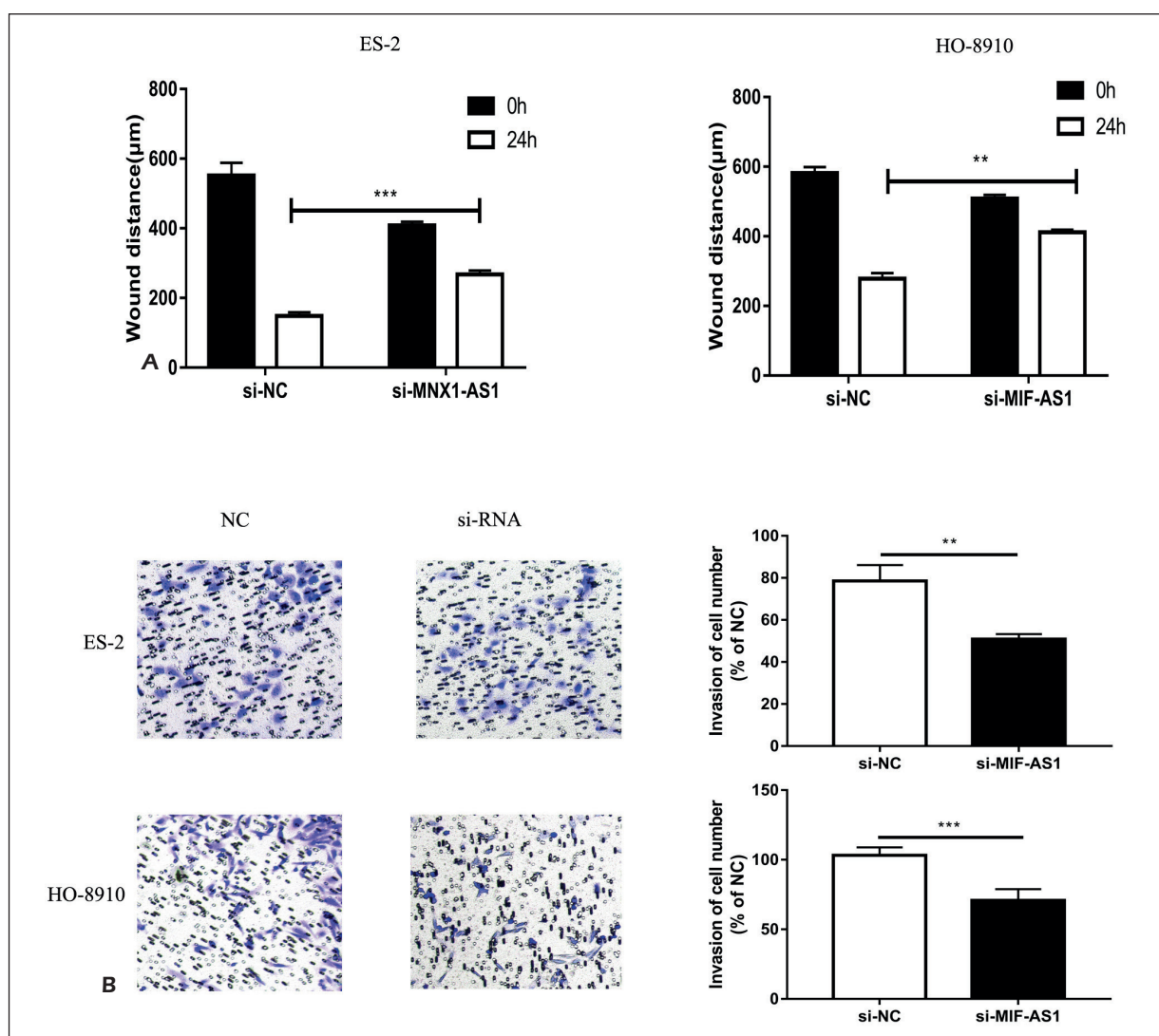


Figure 3. Knockdown of MIF-AS1 suppressed migration and invasion of OC. **A**, Wound distance in HO-8910 and ES-2 cells transfected with si-NC or si-MIF-AS1 (magnification: 20×). **B**, Relative number of invasive cells in HO-8910 and ES-2 cells transfected with si-NC or si-MIF-AS1 (magnification: 20×). ** $p < 0.01$; *** $p < 0.001$.

PLCB1 is a member of the G-protein coupled receptor-associated PLC- β isoform. Catalyzed PLCB2 contributes to form phosphatidylinositol 4,5-diphosphate (PIP2), inositol 1,4,5-triphosphate (IP3), and diacylglycerols (DAG)¹⁸. PLCB1 is up-regulated during carcinogenesis¹⁹. Molinari et al²⁰ have pointed out changes in the copy number of PLCB1 in breast cancer, and its expression level is associated with histological grade and proliferation index. Meanwhile, PLCB1 promotes the malignant progression of tumor cells by activating the ERK pathway in liver cancer²¹. Our findings illustrated that miRNA-31-5p was downregulated, while PLCB1 was upregulated in OC cells. The overexpression of miRNA-31-5p remarkably downregu-

lated PLCB1 expression. Dual-Luciferase reporter gene assay confirmed that the regulatory loop MIF-AS1/miRNA-31-5p/PLCB1 was identified, which accelerated the malignant progression of OC.

Conclusions

In summary, it has been found that MIF-AS1 was significantly upregulated in OC, which accelerated the proliferative, migratory, and invasive abilities of OC cells. Furthermore, the regulatory loop MIF-AS1/miRNA-31-5p/PLCB1 could be utilized as a therapeutic target for OC.

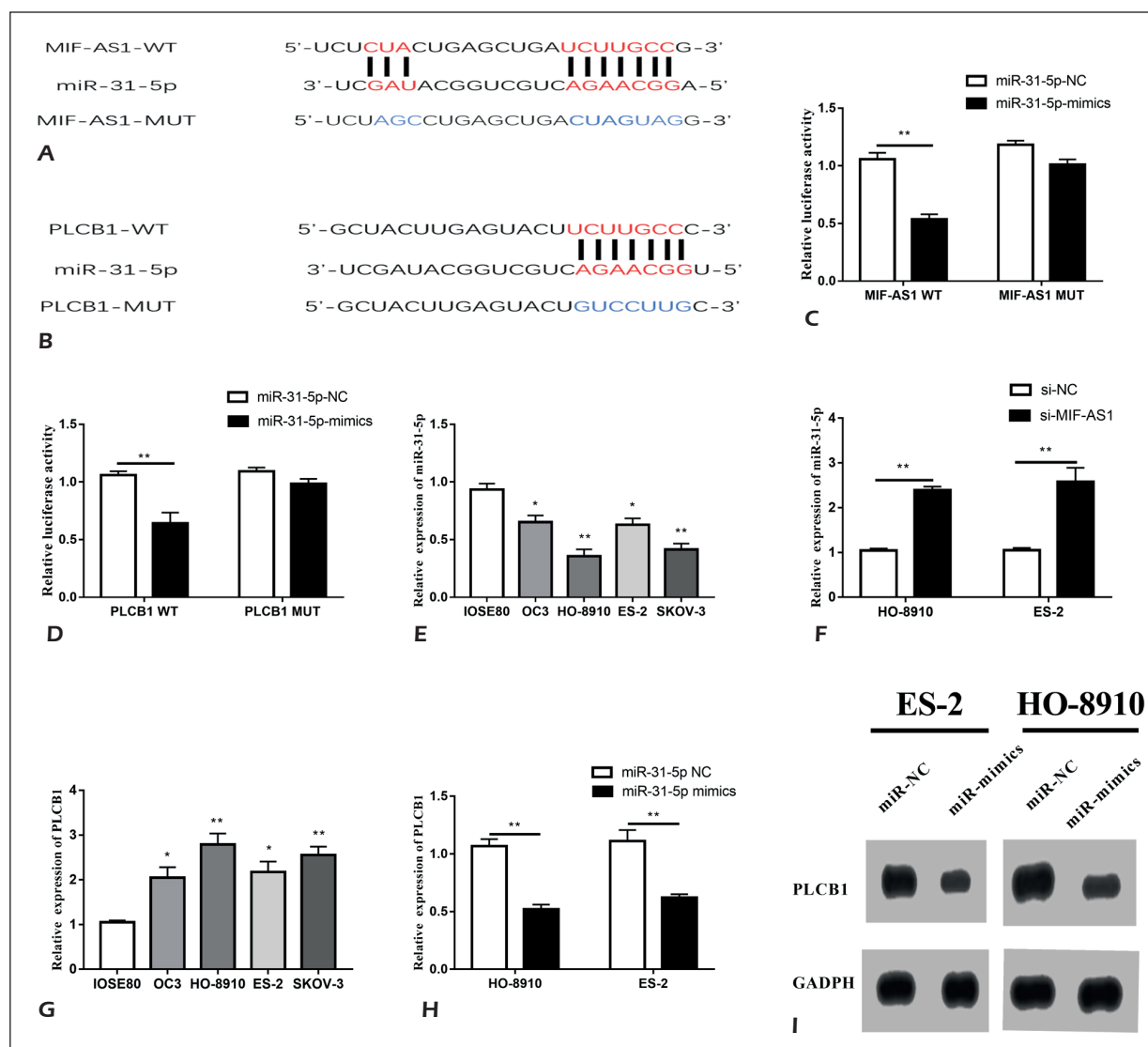


Figure 4. Interaction in MIF-AS1/miRNA-31-5p/PLCB1. **A**, Binding sequences in the promoter regions of MIF-AS1 and miRNA-31-5p. **B**, Binding sequences in the promoter regions of miRNA-31-5p and PLCB1. **C**, Luciferase activity in HO-8910 cells co-transfected with MIF-AS1 WT/MIF-AS1 MUT and miRNA-31-5p mimics/NC. **D**, Luciferase activity in HO-8910 cells co-transfected with PLCB1 WT/PLCB1 MUT and miRNA-31-5p mimics/NC. **E**, MiRNA-31-5p level in ovarian epithelial cells (IOSE80) and OC cells (OC3, HO-8910, ES-2, and SKOV-3). **F**, MiRNA-31-5p level in HO-8910 and ES-2 cells transfected with si-NC or si-MIF-AS1. **G**, PLCB1 level in ovarian epithelial cells (IOSE80) and OC cells (OC3, HO-8910, ES-2, and SKOV-3). **H**, **I**, The mRNA (**H**) and protein (**I**) levels of PLCB1 in HO-8910 and ES-2 cells transfected with negative control or miRNA-31-5p mimics. * $p < 0.05$; ** $p < 0.01$; *** $p < 0.001$.

Conflict of Interests

The authors declare that they have no conflict of interests.

References

1) HOOSSEN Y, PRADEEP P, KUMAR P, DU TOIT LC, CHOONARA YE, PILLAY V. Nanotechnology and glycosaminoglycans: paving the way forward for ovarian cancer intervention. *Int J Mol Sci* 2018; 19. pii: E731.

2) ZHANG Y, ZHANG D, WANG H. Research on correlations of ERCC-1 with proliferation and apoptosis of ovarian cancer cells. *J BUON* 2018; 23: 1753-1795.

3) RUSTIN GJ, VAN DER BURG ME, GRIFFIN CL, GUTHRIE D, LAMONT A, JAYSON GC, KRISTENSEN G, MEDIOLA C, COENS C, QIAN W, PARMAR MK, SWART AM; MRC OV05; EORTC 55955 investigators. Early versus delayed treatment of relapsed ovarian cancer (MRC OV05/EORTC 55955): a randomised trial. *Lancet* 2010; 376: 1155-1163.

- 4) ZHOU H, ZHAO H, LIU H, XU X, DONG X, ZHAO E. Influence of carboplatin on the proliferation and apoptosis of ovarian cancer cells through mTOR/p70s6k signaling pathway. *J BUON* 2018; 23: 1732-1738.
- 5) FRITAH S, NICLOU SP, AZUAJE F. Databases for lncRNAs: a comparative evaluation of emerging tools. *RNA* 2014; 20: 1655-1665.
- 6) WANG K, LIU F, ZHOU LY, LONG B, YUAN SM, WANG Y, LIU CY, SUN T, ZHANG XJ, LI PF. The long noncoding RNA CHR1F regulates cardiac hypertrophy by targeting miR-489. *Circ Res* 2014; 114: 1377-1388.
- 7) LI Y, SYED J, SUGIYAMA H. RNA-DNA triplex formation by long noncoding RNAs. *Cell Chem Biol* 2016; 23: 1325-1333.
- 8) ZHANG Y, ZHANG D, LV J, WANG S, ZHANG Q. LncRNA SNHG15 acts as an oncogene in prostate cancer by regulating miR-338-3p/FKBP1A axis. *Gene* 2019; 705: 44-50.
- 9) ZHAO H, XING G, WANG Y, LUO Z, LIU G, MENG H. Long noncoding RNA HEIH promotes melanoma cell proliferation, migration and invasion via inhibition of miR-200b/a/429. *Biosci Rep* 2017; 37: pii: BSR20170682.
- 10) LIU S, LEI H, LUO F, LI Y, XIE L. The effect of lncRNA HOTAIR on chemoresistance of ovarian cancer through regulation of HOXA7. *Biol Chem* 2018; 399: 485-497.
- 11) LI J, HUANG Y, DENG X, LUO M, WANG X, HU H, LIU C, ZHONG M. Long noncoding RNA H19 promotes transforming growth factor-beta-induced epithelial-mesenchymal transition by acting as a competing endogenous RNA of miR-370-3p in ovarian cancer cells. *Onco Targets Ther* 2018; 11: 427-440.
- 12) WANG L, YU M, ZHAO S. LncRNA MEG3 modified epithelial-mesenchymal transition of ovarian cancer cells by sponging miR-219a-5p and regulating EGFR. *J Cell Biochem* 2019; 120: 17709-17722.
- 13) LI L, LI Y, HUANG Y, OUYANG Y, ZHU Y, WANG Y, GUO X, YUAN Y, GONG K. Long non-coding RNA MIF-AS1 promotes gastric cancer cell proliferation and reduces apoptosis to upregulate NDUFA4. *Cancer Sci* 2018; 109: 3714-3725.
- 14) DING J, WU W, YANG J, WU M. Long non-coding RNA MIF-AS1 promotes breast cancer cell proliferation, migration and EMT process through regulating miR-1249-3p/HOXB8 axis. *Pathol Res Pract* 2019; 215: 152376.
- 15) PUJADE-LAURAIN E, HILPERT F, WEBER B, REUSS A, POVEDA A, KRISTENSEN G, SORIO R, VERGOTE I, WITTEVEEN P, BAMIAS A, PEREIRA D, WIMBERGER P, OAKNIN A, MIRZA MR, FOLLANA P, BOLLAG D, RAY-COQUARD I. Bevacizumab combined with chemotherapy for platinum-resistant recurrent ovarian cancer: the AURELIA open-label randomized phase III trial. *J Clin Oncol* 2014; 32: 1302-1308.
- 16) TAO F, TIAN X, LU M, ZHANG Z. A novel lncRNA, Lnc-OC1, promotes ovarian cancer cell proliferation and migration by sponging miR-34a and miR-34c. *J Genet Genomics* 2018; 45: 137-145.
- 17) BALLANTYNE MD, McDONALD RA, BAKER AH. LncRNA/MicroRNA interactions in the vasculature. *Clin Pharmacol Ther* 2016; 99: 494-501.
- 18) MARTELLI AM, FIUME R, FAENZA I, TABELLINI G, EVANGELISTA C, BORTUL R, FOLLO MY, FALA F, COCCO L. Nuclear phosphoinositide specific phospholipase C (PI-PLC)-beta 1: a central intermediary in nuclear lipid-dependent signal transduction. *Histol Histopathol* 2005; 20: 1251-1260.
- 19) FOLLO MY, MARMIROLI S, FAENZA I, FIUME R, RAMAZZOTTI G, MARTELLI AM, GOBBI P, McCUBREY JA, FINELLI C, MANZOLI FA, COCCO L. Nuclear phospholipase C beta1 signaling, epigenetics and treatments in MDS. *Adv Biol Regul* 2013; 53: 2-7.
- 20) MOLINARI C, MEDRI L, FOLLO MY, PIAZZI M, MARIANI GA, CALISTRI D, COCCO L. PI-PLCβ1 gene copy number alterations in breast cancer. *Oncol Rep* 2012; 27: 403-408.
- 21) LI J, ZHAO X, WANG D, HE W, ZHANG S, CAO W, HUANG Y, WANG L, ZHOU S, LUO K. Up-regulated expression of phospholipase C, beta1 is associated with tumor cell proliferation and poor prognosis in hepatocellular carcinoma. *Onco Targets Ther* 2016; 9: 1697-1706.